pH Dependence of Hydrogen Exchange from Backbone Peptide Amides of Melittin in Methanol

Christopher E. Dempsey

Biochemistry Department, Oxford University, South Parks Road, Oxford OX1 3QU, England

Received September 14, 1987; Revised Manuscript Received May 13, 1988

ABSTRACT: pH-dependent amide exchange rates have been measured for 22 of the 24 exchangeable backbone amides of bee venom melittin in methanol by ^{1}H NMR spectroscopy. pH-dependent exchange rate constants for each amide fitted curves calculated by assuming acid and base catalysis by solvent, indicating that reliable pH-dependent amide exchange data can be obtained from peptides in methanol. The ratio of k_{min}, the rate at the minimum of the pH-dependent exchange curve, to $k_{min(free)}$, the minimum rate for a free amide, is taken to be a measure of the equilibrium constant K_0 for the local structure-opening fluctuation freeing each amide for exchange with solvent. This leads to a model for the structure and conformational stability of melittin in methanol consisting of an N-terminal helical section (residues 1–11) and a more stable C-terminal helix (residues 12–26) with a conformationally labile region around the proline-14 residue in which amides of residues 12, 13, and 15 exchange rapidly with solvent. Similarities in K_0 values among the amides in each helical section indicate that conformational fluctuations involving cooperative breaking of sequential hydrogen bonds may limit amide exchange. The poor correspondence between experimental pH_{min} values, the pH at the minimum of the pH-dependent exchange curves, and the values calculated by incorporating the sequence-dependent inductive contributions of Molday et al. [Molday, R. S., Englander, S. W., & Kallen, R. G. (1972) *Biochemistry 11*, 150–158] indicates that exchange occurs from conformers in which residual conformation-dependent contributions dominate variations in pH_{min} values. Electrostatic contributions from side-chain charges are shown to have a negligible influence on amide exchange, and variations in pH_{min} values are most consistent with a contribution from the effective charges of the helix dipole.

The structure of bee venom melittin (Habermann & Jentsch, 1967) in methanol has recently been determined with two-dimensional proton nuclear magnetic resonance (NMR)[1] spectroscopy and restrained molecular dynamic simulations (Bazzo et al., 1988). Melittin in methanol adopts a helical conformation with a flexible bend in the region of proline-14. Similar conformations have been determined from X-ray diffraction analysis of crystals of tetrameric melittin grown from aqueous solutions at high ionic strength (Terwilliger & Eisenberg, 1982) and are proposed for the structure of the peptide bound to phospholipid bilayer membranes (Dawson et al., 1978; Terwilliger et al., 1982).

In the NMR study, hydrogen exchange measurements were used to identify hydrogen-bonded amides and to define the limits of the melittin helix (Bazzo et al., 1988). More extensive analysis of peptide amide exchange by NMR allows determination of the local stability of hydrogen-bonded secondary structure from which interpretations of the conformational fluctuations limiting amide exchange may be made (Hvidt & Neilsen, 1966; Woodward et al., 1982; Wagner, 1983; Englander & Kallenbach, 1984). Where pH-dependent amide exchange data defining both the acid- and base-catalyzed exchange rate constants and the pH of minimum rate can be obtained, the analysis can be extended to include the contribution of inductive (Molday et al., 1972), electrostatic (Kim & Baldwin, 1982; Matthew & Richards, 1983), and other factors such as amide carbonyl accessibility (Tuchsen & Woodward, 1985) to amide exchange.

In this paper pH-dependent amide exchange data are presented for 22 out of the 24 exchangeable backbone peptide amides of melittin in methanol. It is shown that reliable pH-dependent exchange data can be obtained for polypeptides in methanol. Variations in k_{min}, the slowest exchange rate which occurs at the minimum of the pH-dependent exchange curves, are analyzed in terms of the local stability of hydrogen-bonded secondary structure, and a model for the conformation and structural stability of the peptide in methanol consistent with the NMR-derived structure (Bazzo et al., 1988) is obtained. The pH-dependent exchange data are interpreted to assess the contribution of inductive, electrostatic, and other potential factors that may affect the exchange properties of peptide amides in proteins.

Materials and Methods

Melittin was purified from freeze-dried bee venom (Bulgarcoop, Sofia, Bulgaria) by negative-pressure dialysis, gel filtration on tandem columns of Sephadex G-25 and G-50 (Gauldie et al., 1976), and heparin–Sepharose affinity chromatography (Banks et al., 1981). The assignment of the proton NMR spectrum of melittin in methanol is reported elsewhere (Bazzo et al., 1988).

Time-resolved single amide hydrogen–deuterium exchange experiments (Figure 1) were done as previously described (Dempsey, 1986a), with the Bruker WH 300 NMR spectrometer of the Oxford Enzyme Group. All exchange experiments were done at 20–24 °C, and measured rates were normalized to 20 °C where necessary by using the activation energies for the exchange process determined by Englander et al. (1979). Melittin concentrations of 5 mM were used with no additional buffer ions other than small volumes of meth-

[1] Abbreviations: NMR, nuclear magnetic resonance; BPTI, bovine pancreatic trypsin inhibitor; PDLA, poly(D,L-alanine).

0006-2960/88/0427-6893$01.50/0

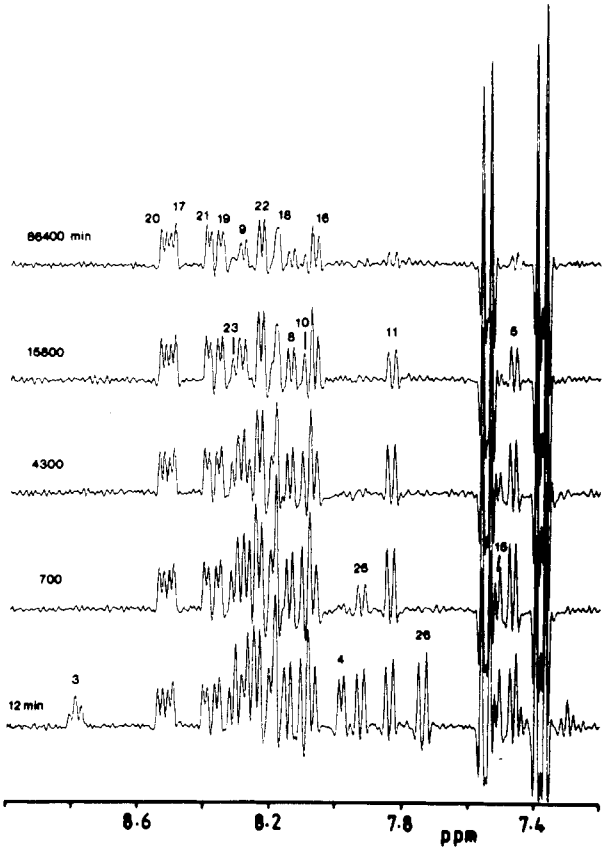

FIGURE 1: Low-field region of the 300-MHz proton NMR spectrum of melittin (5 mM) in deuteriomethanol, pH* 2.6, at increasing time intervals after dissolution. The resolution of the spectra has been enhanced by Gaussian multiplication of the free induction decay. Numbers indicate the amino acid sequence position of assigned amides.

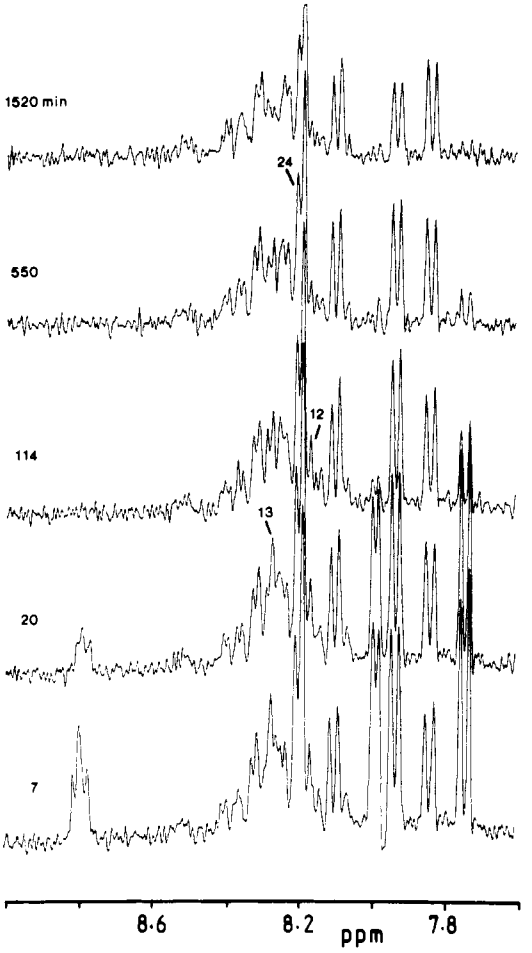

FIGURE 2: Low-field region of the 300-MHz proton NMR spectrum in deuteriomethanol of a sample of melittin where partial exchange-in of rapidly exchanging amides has been achieved as described under Materials and Methods. Amides of residues 12, 13, and 24 are identified.

anolic DCl or NaOD used for pH adjustments. Experiments to test the concentration dependence of amide exchange from melittin in methanol were done with the Bruker 500-MHz spectrometer of the Oxford Enzyme Group.

For selective observation of rapidly exchanging amides, back-exchange experiments (Tuchsen & Woodward, 1985) were performed. In these experiments melittin amides were fully deuteriated by incubating the peptide in D_2O, pH 7.0 at 60 °C for 1 h. The pH was then adjusted to pH 1.0, and the peptide was freeze-dried. Selective in-exchange (deuterium to hydrogen) of rapidly exchanging amides was done by redissolving the peptide in nondeuteriated methanol for 1 h at 20 °C before adding 5 volumes of ice-cold water and rapidly freezing and freeze-drying. Back-exchange at pH 1.0 allowed sufficiently selective protonation of Gly-12 NH and Arg-24 NH (both of which overlap slowly exchanging Ser-18 NH) and Leu-13 NH (overlapping Lys-23 NH; Figure 2) so that out-exchange of these amide protons could be followed by NMR without interference from overlapping signals (Figure 2). Exchange rates of some unresolved amide pairs could be determined by analysis of double-exponential decays where the overlapping amides exchanged with rates differing by a factor of 5 or greater. Twelve to fifteen time points covering at least two half-lives were obtained for the determination of first-order decay constants. Errors in rate measurements were very small and estimated to be always less than 5%.

pH* measurements were made with glass hydrogen combination electrodes (Model CMAWL, Russell pH Electrodes, Auchtermuchty, Scotland) calibrated with aqueous buffers, and pH* values from two different electrodes and meters were averaged to give the values quoted. Independent pH* measurements were within 0.2 pH* unit of one another, and this value is the estimated error in the pH* values quoted in the text. The pH* values are direct pH meter readings uncorrected either for junction potential effects (see Results) or for isotope effects.

pH-dependent exchange data were fitted by a least-square algorithm to curves defined by eq 1 (Leichtling & Klotz, 1966), where k_{ex} is the experimental (pseudo) first-order exchange rate constant, k_D and k_{OMe} are the second-order rate

$$k_{ex} = k_D[D^+] + k_{OMe}[OMe^-] + k_0 \quad (1)$$

constants for acid- and base-catalyzed exchange, and k_0 is the first-order rate constant for pH-independent exchange. Base catalyst[2] concentrations, $[OMe^-]$, were calculated with a value for the dissociation constant of methanol (K_{MeOH}) of $10^{-16.6}$ (Bates, 1973). pH^*_{min} values, where pH^*_{min} is the pH* at the minimum of the pH-dependent exchange curves where $k_D[D^+]$

[2] Because the dissociation constant of water ($K_W = 10^{-14}$) is much greater than that of methanol ($K_{MeOH} = 10^{-16.6}$), the concentration of OD^- should be greater (by 10–15-fold) than the concentration of CD_3O^- even at the very low water concentrations measured in this study (see Results). OD^- from residual water, rather than OMe^-, might therefore be expected to be the dominant exchange catalyst. However, the dissociation of water is highly suppressed in alcoholic solutions (by 100-fold in 80% alcohol to 10^5-fold in solutions approaching pure alcohol; Gutbezahl & Grunwald, 1953). The base catalyst is therefore likely to be the (deuterio)methoxide anion rather than the (deuterio)hydroxide anion.

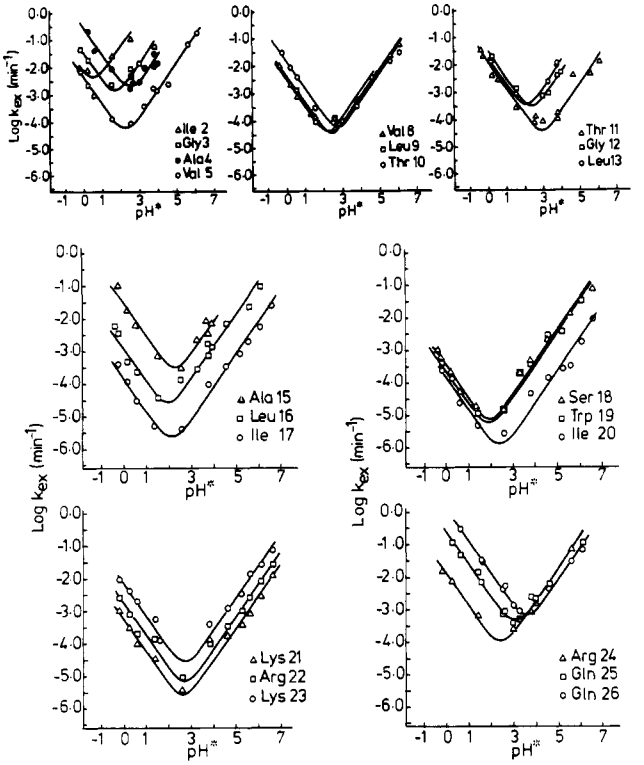

FIGURE 3: pH* dependence of the pseudo-first-order exchange rate constants of individual amides of melittin in deuteriomethanol at 20 °C. Solid lines are least-squares fits to 1 with k_0 equal to zero. pH* values are direct meter readings using a hydrogen electrode calibrated with aqueous pH standards.

$= k_{OMe}[OMe^-]$, were calculated with (Leichtling & Klotz, 1966)

$$pH_{min} = (1/2)[pK_{MeOD} - \log (k_{OMe}/k_D)] \quad (2)$$

RESULTS

pH Measurements in Deuteriomethanol. Junction potential effects complicate the measurement of pH in organic solvents (Bates, 1973). To determine the reliability of pH* measurements in methanol with a glass electrode calibrated with aqueous buffers, pH-titration data were obtained for model peptides in that solvent. The titration data could be well fitted to the Henderson–Hasselbach equation (e.g., glycyllysine: pK_a of α-carboxyl = 5.1, pK_a of N^{α}-amine = 6.8, and pK_a of N^{ϵ}-amine = 10.1 in CD_3OD determined from pH-dependent NMR chemical shift variations) indicating that the apparent pH (pH*) is a linear function of the true deuteron ion activity (data not shown). Similarly, the good fits of the pH-dependent exchange data for melittin amides in CD_3OD (Figure 3) support the validity of the pH* measurements.

Douheret (1967) has determined the difference, due to the junction potential artifact, between pH* and the true pH for water–methanol mixtures. For the lowest concentration of water in methanol reported, 93.8 mol % methanol in water, pH* is 0.62 pH unit lower than the true pH. Rather lower water concentrations were found in the exchange samples in this study (96–98 mol % methanol; determined by integrating the residual protonated solvent resonance in the proton NMR spectrum of melittin–CD_3OD exchange samples) so that pH* may be somewhat greater than 0.62 pH unit lower than the true pH (de Ligny et al., 1960). In comparing differences in pH-dependent parameters among the amides in melittin, these considerations are not important because data for each amide within a single exchange sample are equally affected by the junction potential artifact. However, variations in water content among *different* exchange samples can result in large variations in the difference between $pH_{(true)}$ and pH*, particularly at very low water concentrations (de Ligny et al., 1960; Bates et al., 1963). Such differences seem to be largely compensated by changes in the acid and base catalyst activities as shown by exchange experiments done with the addition of small volumes of added water (Figure 4). In the experiment illustrated in Figure 4, addition of water resulted in large shifts in pH* (from pH* 1.4 at 98% CD_3OD to pH* 2.1 at 96.5% CD_3OD to pH* 2.4 at 95% CD_3OD for the sample studied), but the exchange rates of the amides measured varied so that they remained on the pH-dependent exchange curves determined without the addition of water. This effect is not completely understood but seems to underlie the reliability of the pH-dependent exchange data that were obtained without taking particular care to ensure identical residual water concentrations among exchange samples.

pH-Dependent Amide Exchange. Of the 24 peptide amide protons in melittin, pH-dependent exchange data could be

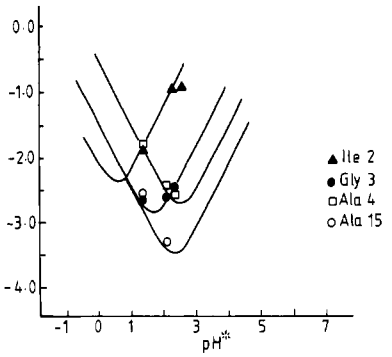

FIGURE 4: Effect of varying the water content on the exchange rate constants of individual amides of melittin in deuteriomethanol containing 2 mol % D_2O (points at pH* 1.4), 3.5 mol % D_2O (pH* 2.1), and 5 mol % D_2O (pH* 2.4). Solid lines are taken from Figure 3.

Table I: Hydrogen Exchange Parameters for Melittin Amides in Methanol

amide	k_D (M^{-1} min^{-1})	k_{OMe} (M^{-1} min^{-1})	k_{OMe}(MEK)[a]	pH^*_{min}
Ile-2	7.6×10^{-3}	2.4×10^{13}	8.2×10^{11}	0.55
Gly-3	3.4×10^{-2}	5.8×10^{11}	1.2×10^{11}	1.68
Ala-4	3.1×10^{-1}	1.2×10^{11}	1.2×10^{11}	2.50
Val-5	4.8×10^{-3}	6.4×10^{9}	6.4×10^{9}	2.25
Leu-6	ND[b]	ND	ND	
Lys-7	ND	ND	ND	
Val-8	4.6×10^{-3}	3.2×10^{9}	1.6×10^{9}	2.38
Leu-9	3.6×10^{-3}	5.0×10^{9}	5.0×10^{9}	2.23
Thr-10	1.8×10^{-2}	2.2×10^{9}	7.0×10^{8}	2.76
Thr-11	1.6×10^{-2}	8.5×10^{8}	1.4×10^{8}	2.94
Gly-12	3.7×10^{-2}	2.4×10^{10}	4.2×10^{9}	2.40
Leu-13	2.1×10^{-2}	6.6×10^{10}	3.0×10^{10}	2.08
Ala-15	3.2×10^{-2}	3.3×10^{10}	3.3×10^{10}	2.30
Leu-16	1.3×10^{-3}	5.5×10^{9}	5.5×10^{9}	2.00
Ile-17	1.7×10^{-4}	3.3×10^{8}	3.3×10^{8}	2.15
Ser-18	3.6×10^{-4}	1.6×10^{9}	5.1×10^{8}	1.97
Trp-19	2.4×10^{-4}	1.4×10^{9}	8.9×10^{8}	1.92
Ile-20	1.6×10^{-4}	1.0×10^{8}	7.8×10^{7}	2.41
Lys-21	5.9×10^{-4}	1.4×10^{8}	1.1×10^{8}	2.61
Arg-22	1.9×10^{-3}	3.2×10^{8}	1.3×10^{8}	2.68
Lys-23	7.6×10^{-3}	1.2×10^{9}	4.7×10^{8}	2.71
Arg-24	1.3×10^{-2}	7.6×10^{9}	3.1×10^{9}	2.41
Gln-25	2.5×10^{-1}	7.4×10^{9}	1.5×10^{9}	3.07
Gln-26	1.3	3.6×10^{9}	1.8×10^{9}	3.60

[a] Base-catalyzed exchange rate constants corrected for sequence-dependent inductive effects according to the empirical rules of Molday et al. (1972). The inductive contribution of Trp to exchange of adjacent peptide amides is not listed in the data of Molday et al. (1972) and is assumed here to have the same contribution as Tyr. [b] ND, not determined.

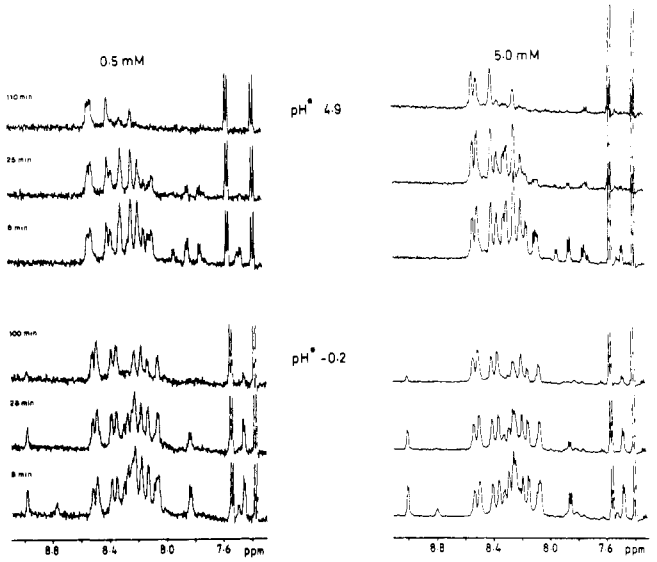

FIGURE 5: Amide exchange from melittin amides in deuteriomethanol under conditions of acid catalysis (pH* −0.2; lower spectra) and base catalysis (pH* 4.9; upper spectra) at melittin concentrations of 0.5 mM (left-hand series of spectra) and 5 mM (right-hand series). Comparison of pairs of spectra across the figure shows that there is little variation of either the amide chemical shifts or exchange rates with variation of peptide concentration at either pH.

obtained for 22 amides for the satisfactory determination of values of k_D, k_{OMe}, and pH^*_{min} and to evaluate the pH dependence of acid- and base-catalyzed exchange rate constants. The pH dependence of amide exchange for individual amides is shown in Figure 3, and the exchange parameters extracted from these data are given in Table I. Leu-6 NH and Lys-7 NH could not be resolved at 300 MHz, and data for these amides are lacking. Spectral overlap in the amide region of the 300-MHz proton spectrum limited the data obtainable for the amides of Leu-9, Gly-12, Leu-13, and Arg-24 to six points. All exchange data for Gly-12 NH and some for Leu-13 and Arg-24 NH's were obtained from back-exchange experiments (Tuchsen & Woodward, 1985; Figure 2) as described under Materials and Methods.

The pH dependence of the pseudo-first-order hydrogen–deuterium exchange rate constants for all the melittin amides could be well fitted to eq 1 (Figure 3). Satisfactory fits were obtained by setting k_0, the pH-independent exchange rate constant, to zero. For each amide a linear dependence of log k with respect to pH* was found in both the acid- and base-catalyzed regions of the exchange curves. This is consistent with the absence of titratable groups in melittin having pK_a's below pH* 7 in methanol. Titration of charged groups induces deviations from a linear dependence on pH through direct charge effects on the chemical exchange step (Englander & Kallenbach, 1984) or indirectly through "allosteric" effects on local structural stability (Englander & Kallenbach, 1984; Dempsey, 1986a).

Concentration Dependence of Amide Exchange from Melittin in Methanol. To test the possibility that some features of amide exchange from melittin in methanol might be affected by self-association of the peptide in solution, the concentration dependence of exchange was tested at pH* values where either acid catalysis (pH* −0.2), or base catalysis (pH* 4.9) is dominant. At neither pH* was there any significant difference either in the rank order of exchange of different backbone amides or in their absolute rates when exchange experiments were done at melittin concentrations of 0.5 or 5 mM (illustrated in Figure 5). There are no amino group titrations in methanolic solutions of melittin with pK_a's below pH* 7 (C. E. Dempsey and G. D. Cryer, unpublished results), so that the absence of concentration-dependent effects on the exchange properties will apply at least over this range of pH* values (between pH* −0.2 and pH* 4.9). Similarly, the backbone amide protons of melittin in methanol have essentially constant NMR chemical shifts (within 0.01 ppm = 5 Hz at 500 MHz) over the same 10-fold range of concentrations (data not shown), indicating the absence of concentration-dependent effects on conformation. These results support the conclusion that self-association of melittin is not a factor influencing the pH-dependent amide exchange properties.

Analysis of Amide Exchange Data. The slowing of amide exchange of melittin amides in methanol follows the pattern expected for amide protons hydrogen bonded within an α-helix (see Discussion), consistent with the recent NMR structure determination of melittin in methanol (Bazzo et al., 1988). With the assumption that hydrogen-bond breaking is required for exchange with solvent to occur, the exchange process can be described by the usual scheme in which conformational fluctuations occur between native (N) conformers and "open" (O) conformers in which the hydrogen bond is broken, freeing the amide for exchange with solvent (Hvidt & Neilsen, 1966; Englander & Kallenbach, 1984):

$$N(H) \underset{k_2}{\overset{k_1}{\rightleftharpoons}} O(H) \xrightarrow{k_3} O(D) \underset{k_1}{\overset{k_2}{\rightleftharpoons}} N(D) \qquad (3)$$

No assumption is made here about the nature of the conformational fluctuation other than the requirement for hydrogen-bond rupture and exposure of the amide for exchange with solvent.

Pseudo-first-order exchange rate constants for melittin amides follow first order dependence on acid and base catalyst concentration (Figure 3) indicating that amide exchange follows the EX_2 mechanism in which the fluctuations limiting exchange are in preequilibrium with the chemical exchange event (Hvidt & Neilsen, 1966). In the EX_2 limit, the first-order exchange rate constant k_{ex} is given by

$$k_{ex} = (k_1/k_2)k_3 = K_0k_3 \qquad (4)$$

Knowing k_3, the intrinsic exchange rate constant for the amide in consideration, a value of K_0, the equilibrium constant for the exchange-limiting structure-opening fluctuation, can be determined. A comparison of K_0 values for fluctuations limiting exchange of individual amides gives information of local backbone stability throughout the molecule.

Values of k_3 are normally determined by incorporating the sequence-dependent chemical inductive contributions determined by Molday et al. (1972). This approach is often necessary in studies of amide exchange from proteins where rates may be obtainable at only one or a few pH values in the base-catalyzed region. However, while eq 3 describes the amide exchange process in a manner independent of the nature of the exchange-limiting fluctuations involved, the use of only the Molday factors to determine k_3 implicitly assumes that the amides exchange from a conformation equivalent to a "random coil" in which *only* sequence-dependent inductive effects influence amide exchange in the open conformation. A number of factors including both global (Kim & Baldwin, 1982) and local (Matthew & Richards, 1983) electrostatic effects and the accessibility of amide N and O atoms (Tuchsen & Woodward, 1985) are known to have large effects on amide exchange and might have residual influence on k_3 if exchange-limiting fluctuations do not yield local open structures that are essentially random coil.

An alternative approach for determining K_0 values is possible where pH-dependent exchange data in both the acid- and

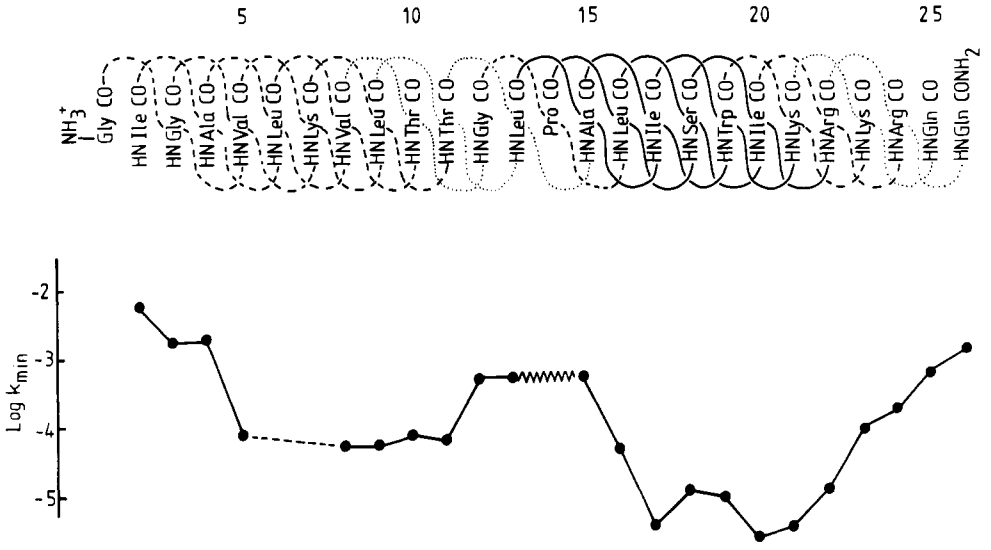

FIGURE 6: log k_{min} values as a function of amino acid sequence of individual amides in melittin in deuteriomethanol at 20 °C. The proposed hydrogen-bond pattern is illustrated schematically in the top of the figure with the density of lines denoting the relative stability of hydrogen bonds as determined from the k_{min} values.

base-catalyzed exchange regions are obtained. The ratio $k_{min}/k_{min(free)}$, where k_{min} is the exchange rate at the minimum of the pH-dependent exchange curve and $k_{min(free)}$ is k_{min} for a non-hydrogen-bonded amide free to exchange with solvent, can be used as a direct measure of K_0. This relationship is valid with the assumption that inductive, electrostatic, and other factors affecting k_D and k_{OMe} alter the acid- and base-catalyzed rate constants in approximately equal and opposite ways (Molday et al., 1972) and thus shift the pH-dependent exchange curves with respect to pH without greatly affecting k_{min} (Leichtling & Klotz, 1966). This approach is used here.

Large variations in k_{min} are observed among the melittin amides, and these values are plotted (as log k_{min}) against residue number in Figure 6. A schematic illustration of the hydrogen-bond pattern for an α-helix in melittin is also shown in Figure 6, and the stability of each amide to exchange, determined from the k_{min} values, is indicated by the density of the line designating each hydrogen bond.

The amides of residues 2–4 are not hydrogen bonded (see Discussion), and k_{min} for Gly-3 and Ala-4 amide protons is used as $k_{min(free)}$. Val-5 NH has a k_{min} value suppressed by a factor of about 30, and similar slowing factors are observed for sequential amides in the sequence up to Thr-11 NH. Gly-12, Leu-13, and Ala-15 NH have k_{min} values equally suppressed by 5–8-fold compared with the values of the free amides at the N-terminus, and the C-terminal residues have slowing factors of 30-fold (Leu-16) to 200–1000-fold (Ile-17 to Arg-22 NH). Exchange slowing factors tail off steadily toward the C-terminus from Arg-22 NH (Figure 6).

pH^*_{min} Values. Sequence-dependent inductive contributions, acting through bonds, are expected to be similar for peptides in methanol and in water. pH^*_{min} values for the melittin amides calculated with the empirical data of Molday et al. (1972) are compared in Figure 7 with the experimental values extracted from the pH-dependent exchange data of Figure 3. pH^*_{min} for a free amide under the conditions of the exchange experiments in methanol is taken to be pH* 2.5, the pH^*_{min} for Ala-4 NH which is neither hydrogen bonded nor expected to be affected by sequence-dependent inductive effects. Apart from the agreement at the N-terminus where the inductive effect of the N^{α}-amino group dominates variations in pH^*_{min} (Molday et al., 1972), there is little correlation between experimental values and calculated pH^*_{min} values, and this

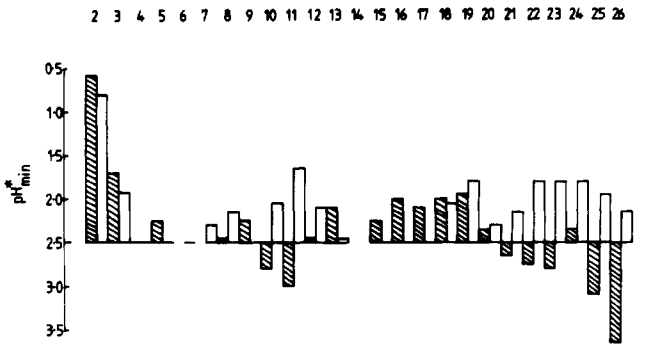

FIGURE 7: Comparison of experimental pH^*_{min} values (hatched bars) for melittin amides in deuteriomethanol with pH^*_{min} values calculated by incorporating sequence-dependent contributions of Molday et al. (1972) (open bars).

conclusion is not altered if a slightly different value for $pH^*_{min(free)}$ is used.

A second potential contribution to variations in pH^*_{min} is the electrostatic field at the amide arising from the side-chain fixed charges (Matthew & Richards, 1982). An estimate of the energy of interaction (W_{ij}) between a proton exchange catalyst localized either at the amide nitrogen or at the carbonyl oxygen and the electrostatic field from the fixed charges was made with (Matthew et al., 1985; Atkins, 1986)

$$W_{ij} = \sum Z_i Z_j q^2 / 4\pi r \epsilon \epsilon_0 \qquad (5)$$

where ϵ_0 is the vacuum permittivity (8.85×10^{-12} J^{-1} C^2 m^{-1}), ϵ, is the dielectric constant of methanol (31) (Bates, 1973), and r is the separation between each side-chain charge and the site of amide protonation (amide N or O). Z_i and Z_j both have a value of +1 for a proton exchange catalyst and positively charged side chains, and q is the electron charge. Distances were measured from a Minit molecular model (Cochranes, Oxford, U.K.) by assuming an α-helical structure for melittin (Bazzo et al., 1988; see Discussion) and an extended fixed conformation for the charged side chains projecting radially from the helix axis (Terwilliger et al., 1982). Amides in a greater positive potential field should have pH^*_{min} values suppressed to lower pH* due to the suppression of acid-catalyzed exchange and the promotion of base-catalyzed exchange. A comparison of the estimated interaction energy for protonation at the nitrogen and carbonyl oxygen of each

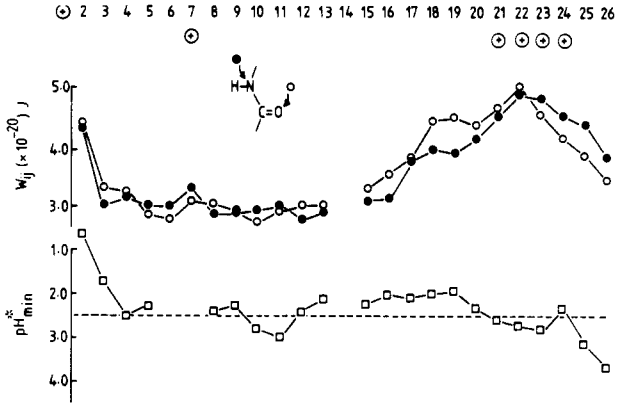

FIGURE 8: Estimation of the electrostatic energy for interaction between a proton exchange catalyst localized either at the amide N (●) or carbonyl O (○) and the electrostatic field arising from side-chain fixed charges of melittin, assuming a helical conformation with side chains extending radially from the helix axis. The experimental pH^*_{min} values (□) are shown below for comparison. The dotted line indicates pH^*_{min} for a non-hydrogen-bonded amide expected to be unaffected by sequence-dependent inductive effects (Ala-4 NH). See text for details.

amide, with the experimental pH^*_{min} values, is shown in Figure 8. Interaction energies involving protonation at both amide carbonyl and nitrogen were estimated to determine whether electrostatic contributions to variations in pH^*_{min} values among the melittin amides could be better accounted for in one or the other of the mechanisms for acid-catalyzed exchange (exchange-limiting protonation at either O or N; Perrin & Lollo, 1984). In neither case does the estimated electrostatic contribution account for the variations in experimental pH^*_{min} values (Figure 8). In particular, shifts of pH^*_{min} values to high pH* are observed for the C-terminal amides of melittin rather than the shifts to low pH* expected from the influence of the large positive potential field from the four positively charged amino acids in the C-terminal sequence (Figure 8).

Discussion

pH-Dependent Amide Exchange in Methanol. The excellent fit to eq 1 of the experimental exchange data for individual amides in melittin (Figure 3) indicates that reliable pH-dependent exchange data can be obtained for polypeptides in methanol. The large variations in the liquid junction potential that occur when the hydrogen electrode is used for pH measurements in methanol at very low water concentrations (de Ligny et al., 1960; Bates, 1973) do not cause large errors in the pH-dependent exchange data apparently because small variations in water content (that do cause large variations in pH*) are compensated by changes in the activities of the acid and base exchange catalysts (Figure 4). The measured pH (pH*) in methanol using the glass electrode calibrated with aqueous buffers is not a true measure of the hydrogen ion concentration because of junction potential effects. For this reason, as well as probable inaccuracies in the value of K_{MeOD} (from which $[CD_3O^-]$ is calculated), the k_D and k_{OMe} values must be considered "apparent" values. This is the reason, for example, that the apparent k_{OD} for Ile-2 NH, 4×10^{13} M^{-1} min^{-1}, is faster than the diffusion-limited rate for base-catalyzed exchange in water at 20 °C ($\sim 1 \times 10^{12}$ M^{-1} min^{-1}) estimated by Molday and Kallen (1972).

These considerations do not adversly affect comparison of exchange parameters among the melittin amides because data from each amide within a single sample are equally affected by junction potential effects or inaccuracies in K_{MeOD}. Moreover, the exchange parameters for non-hydrogen-bonded

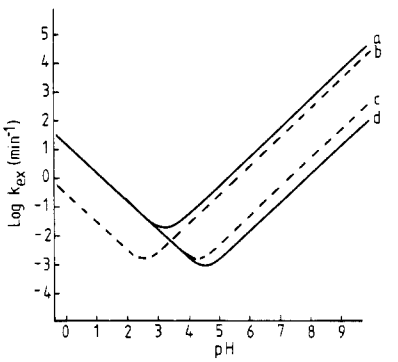

FIGURE 9: pH-dependent amide exchange curves for PDLA (solid lines) in water determined from the data of Englander et al. (1979) (a) and the curve for PDLA expected in methanol if k_D and k_{OD} have the same values in methanol as in water (d). Broken lines are the experimental pH-dependent curve for Ala-4 NH of melittin in methanol (b) and the curve obtained by correcting for junction potential and global charge effects (see text) by assuming k_D for Ala-4 NH equals k_D for PDLA (c).

amides in melittin can be well accounted for by comparison with exchange data for amides in water (Figure 9). Thus, k_{min} for non-H-bonded amides (e.g., Ala-4 NH; $k_{min} = 2 \times 10^{-3}$ min^{-1} at 20 °C; curve b) is about 15-fold slower than k_{min} for poly(D,L-alanine) (PDLA) in water (curve a), a factor consistent with the decrease in total catalyst concentration due to the low dissociation constant of methanol [the expected decrease in k_{min} due to the decrease catalyst concentration in methanol compared with water is $10^{(16.6-14)/2} = 20$-fold].[3] The pH_{min} for PDLA in water is pH 3.1 (Englander et al., 1979) and would be expected to be about pH 4.4 (curve d) in methanol [a result of the decreased dissociation constant for methanol compared with water and the use of pD and K_{MeOD} for determining pOMe; see Englander and Kallenbach (1984), p 565]. The suppressed pH_{min} for Ala-4 NH (pH_{min} is pH* 2.5), for example, is due to the junction potential artifact (around 0.6–1.5 pH units) and the global charge effect arising from the positively charged side chains of melittin that acts to increase the local concentration of CD_3O^- as counterions (Kin & Baldwin, 1982). If the pH-dependent exchange curve for Ala-4 NH (curve b) is shifted along the pH axis to higher pH* to correct for these two effects under the assumption that k_D for Ala-4 NH in methanol is equal to k_D for PDLA in water, then the resulting exchange curve (curve c) is close to that expected for PDLA in methanol (Figure 9). These results suggest that k_D and k_{OMe} (or at least their product) for exchange of a free amide in methanol may be similar to the values of the corresponding exchange rate constants in water and indicate that additional factors peculiar to amide exchange in methanol need not be considered when pH-dependent exchange data in that solvent are analyzed.

Amide Exchange from Melittin in Methanol. The amide exchange data strongly support the interpretation of an extended helical conformation for melittin in methanol (Bazzo et al., 1988). Val-5 NH, the first amide expected to be hydrogen-bonded in an α-helix, has a k_{min} suppressed by about 30-fold relative to the amides of residues Ile-2, Gly-3, and Ala-4 (Figure 6); the large exchange slowing factor is consistent with a hydrogen bond between the Ala-5 NH and the Gly-1 amide carbonyl. Helical hydrogen bonds involving the

[3] The values for K_{H_2O} and K_{MeOH} are used in this calculation rather than those for K_{D_2O} and K_{MeOD}, but it is likely that the difference in the logarithms of the dissociation constants for the deuteriated species will be similar to that for the protonated species.

amide protons of residues Leu-6 to Thr-11 would account for the similar slowing factors of these amides.[4] Stable hydrogen bonds are not formed by the amide protons of Gly-12, Leu-13 and Ala-15 which have exchange slowing factors of only 5–8-fold relative to those of free amides. Helical hydrogen bonds involving these amides are destabilized presumably by the loss of the Pro-14 NH to Thr-10 carbonyl H-bond and the distortions required to accommodate a proline in the helix (Terwilliger et al., 1982; Fox & Richards, 1982; Bazzo et al., 1988).

Very stable hydrogen bonds, characterized by exchange slowing factors of 30–1000, exist at the C-terminal part of the molecule, and the pattern of slowing factors is also consistent with a helical conformation. Particularly stable are hydrogen bonds involving the amide protons of residues Ile-17 through Arg-22 with the backbone amide carbonyls of (for an α-helix) Leu-13 to Ser-18. Increasing k_{min} values (Figure 6) are found sequentially from Arg-22 NH to Gln-26 at the C-terminus, the latter amide exchanging almost as quickly as the free amides at the N-terminus. This "helix-fraying" behavior has been observed in amide exchange studies of other peptides and proteins (Kuwajima & Baldwin, 1983; Wemmer & Kallenbach, 1983; Dempsey, 1986a; Wand et al., 1986) and is predicted in theories of helix–coil transitions in polypeptides (Schellman, 1955).

As outlined under Results, the ratio of k_{min} for a hydrogen-bonded amide to k_{min} for a non-hydrogen-bonded amide free to exchange with solvent [$k_{min(free)}$] is taken as a direct measure of the equilibrium constant, K_0, for the transition between the "closed" and "open" conformations in the unit of secondary structure containing the hydrogen-bonded amide. Within this model, quantitative determination of the relative stability of local hydrogen-bonded conformation in the peptide backbone and interpretations about the nature of the conformational fluctuations may be made. The melittin structure in methanol can be seen to consist of two helical regions having independent fluctuational properties. The N-terminal helical segment (comprising the first 11 amino acids of the peptide) is around 30 times less stable than the C-terminal helix, and amide exchange from the N-terminal helix must occur through local fluctuations that do not involve the C-terminal helix. The constancy of slowing factors for amides along the N-terminal helix (Figure 6) suggests that concerted opening fluctuations of the helix limit the exchange of these amides. This conclusion cannot, however, be proved from amide exchange measurements in the EX_2 limit, and separate exchange-limiting opening of individual helical hydrogen bonds is also consistent with the exchange data.

The small but constant exchange slowing factors for the protons of Gly-12, Leu-13, and Ala-15 (Figure 6) are consistent with a concerted opening of the distorted turn of helix containing the hydrogen bonds involving these amides. The significance of differences in log k_{min} values in the C-terminal helix is more difficult to evaluate. Although the similar (200–1000-fold) slowing factors for the amide protons in the sequence Ile-17 to Arg-22 may indicate concerted fluctuations of the stable region of the C-terminal helix, the amides of Ser-18 and Trp-19 exchange about five times faster than the other amides in this sequence (Figure 6), a factor which is reflected in both the k_D and k_{OMe} values (Table I). If differences in k_{min} values are taken literally as a measure of the equilibrium constant between the hydrogen-bonded "closed" form and the "open" form, then an additional independent structural fluctuation can be postulated to allow exchange of these amides. The hydrogen bonds involving Ser-18 and Trp-19 NH (with the carbonyls of Pro-14 and Ala-15) lie on the external face of the helix bend (Terwilliger et al., 1982; Bazzo et al., 1988) where helix distortions (expansion) are likely to promote more rapid exchange than on the internal face where the helical structure may be compressed as observed in amphipathic helices in other proteins (Blundell et al., 1983; Wagner et al., 1984).

Helix fraying in the C-terminal helix of melittin in methanol is characterized by sequential increases in k_{min} of 3–5-fold from Arg-22 NH to Gln-26 NH. Suprisingly, no helix fraying is apparent at the N-terminus of the melittin molecule, the first hydrogen bond (Ala-5 NH to Gly-1 C=O) being as stable as subsequent helical hydrogen bonds in the N-terminal helix (Figure 6) whether k_{min}, k_D, or k_{OMe} values are considered (Table I).

The enhanced *overall* stability of the C-terminal helical section (Figure 6) may result from the increased number of hydrogen bonds (12) compared to the N-terminal helix (9 hydrogen bonds) or to greater helix-forming tendency of amino acids in this helix. With use of the Chou and Fasman parameters for predicting secondary structure in polypeptide sequences (Chou & Fasman, 1974b), the N-terminal sequence of melittin is more strongly predicted to be helical than the C-terminal sequence [residues 1–11, $\langle P_\alpha \rangle$ = 1.02; residues 2–11, $\langle P_\alpha \rangle$ = 1.07; residues 12–26, $\langle P_\alpha \rangle$ = 1.02; residues 13–26, $\langle P_\alpha \rangle$ = 1.05; inner helical residues (Chou & Fasman, 1974a) 4–9, $\langle P_\alpha \rangle$ = 1.25; residues 15–23, $\langle P_\alpha \rangle$ = 1.07]. The increased number of helical hydrogen bonds in the C-terminal helix may therefore be the origin of high stability of that helix in agreement with theoretical (Schellman, 1955; Creighton, 1983) and experimental treatments (Nakanishi et al., 1972) of the cooperativity of hydrogen bonding in peptide helices.

A model for the conformational properties of melittin in methanol interpreted with K_0 values determined from k_{OMe} after correcting for sequence-dependent inductive effects is similar to that described above using $k_{min}/k_{min(free)}$ as a measure of K_0 (as can be seen by inspection of corrected K_{OMe} values in Table I) but lacks the marked similarity in slowing factors in the N-terminal helical section and contains a C-terminal helix where helix-fraying stops abruptly at residue 24. Without an independent measure of "true" K_0 values, it is not possible to be certain that either model is completely correct.

pH_{min}. Sequence-dependent inductive effects modulate pH_{min} values in pH-dependent amide exchange from polypeptides by altering the stability of acid- and base-catalyzed exchange intermediates. These effects have been calibrated by Molday et al. (1972), and the correction factors are often used to normalize measured exchange rates at a given pH to the rate for a free amide [poly(D,L-alanine)] at that pH to increase the accuracy of interpretations of fluctuational modes limiting amide exchange (Kuwajima & Baldwin, 1983; Wagner et al., 1984; Vasent Kumar & Kallenbach, 1985; Wand et al., 1985; Henry et al., 1987). Amides exchanging from a "random-coil" conformation should have pH_{min} values identical with those calculated from the data of Molday et al. (1972) if global charge effects (Kim & Baldwin, 1982) are taken into account (Leichtling & Klotz, 1966; Dempsey, 1986a). In the three studies in which experimental pH_{min} values have been compared with pH_{min} values calculated by incorporating the sequence-dependent inductive contributions

[4] Although pH-dependent exchange data were not obtained for the Leu-6 and Lys-7 amide protons, 2D NMR experiments done at 500 MHz under conditions of partial amide exchange showed that these amides were equally protected from exchange as the other amides in the N-terminal section of melittin at pH* 3.2.

of Molday et al. (1972), poor correlations are observed in each case (Tuchsen & Woodward, 1985; Dempsey, 1986a; this study).

Although it is likely that sequence-dependent inductive contributions do apply to exchange in polypeptides, their effects on acid- and base-catalyzed exchange (and thus pH_{min}) seem to be outweighed by other factors. The conclusion seems to be that whatever conformational fluctuations are limiting for amide exchange (in these examples) these fluctuations do not lead to local "random-coil" states in which only sequence-dependent contributions to amide exchange apply (Dempsey, 1986b). Residual conformation-dependent contributions were shown for surface amides in BPTI to arise from the *local* electrostatic fields from side-chain fixed charges and the accessibility of the amide carbonyl that affects acid-catalyzed exchange through the imidic acid mechanism (Tuchsen & Woodward, 1985). The ability to account for these contributions by comparison with the crystal structure indicates that the surface amides of BPTI exchange from a conformation similar to the native conformation. Exchange of stable amides in apamin was proposed to occur through concerted opening of hydrogen-bonded secondary structure, and the poor correlation of measured and calculated pH_{min} values was attributed to residual conformation in the open conformers from which exchange occurred (Dempsey, 1986a).

The first of these factors, the electrostatic fields arising from side-chain fixed charges in melittin, can be ruled out as a significant factor in modulating pH^*_{min} values for amide exchange in melittin. There is no suppression of pH^*_{min} values to low pH for amides in the C-terminal region of melittin that would be expected if local electrostatic fields arising from charged side chains in the sequence Lys-Arg-Lys-Arg were important (Figure 8). The absence of local electrostatic contributions from side-chain charges on amide exchange in melittin is probably a result of the high solvent accessibility of these charges resulting in their effective neutralization by counterions and the solvent dielectric (Matthew & Richards, 1982).

The marked pattern of k_{min} values in the C-terminal region of melittin, where the N-terminal amides (Ala-15 NH to Thr-19 NH) have low pH^*_{min} values with subsequent amides having pH^*_{min} values increasing regularly toward the C-terminus, is opposite to predictions based on sequence-dependent inductive effects (Figure 7) or electrostatic contributions from side-chain charges (Figure 8). A similar pattern of low pH^*_{min} values at the N-terminus and high pH^*_{min} values at the C-terminal end of the N-terminal helix is also apparent (Figure 7). This distribution of pH^*_{min} values is similar to that expected due to the effective charges arising from the helix dipole (Hol, 1985). The localization of an effective negative charge at the C-terminal end of the melittin helix would induce shifts of pH^*_{min} to high pH* toward the C-terminus whereas shifts of pH^*_{min} to low pH* would occur at the N-terminal end of the helix due to the effective positive charge from the helix dipole as observed (Figure 7). This interpretation requires that the two helical sections are independent to the extent that the effective dipole charges at the C-terminal end of the N-terminal helix and the N-terminal end of the C-terminal helix do not cancel one another.

Variations in pH^*_{min} values among the melittin amides may also have a contribution from amide carbonyl accessibilities, those amides having high solvent accessibility exhibiting enhanced acid-catalyzed exchange and thus enhanced pH_{min} values (Tuchsen & Woodward, 1985). The relative contribution of these two factors (helix dipole effective charges and carbonyl accessibility) cannot be assessed from the data presented here, although little variation in carbonyl accessibility might be expected in a relatively small, monomeric, helical peptide in solution. Nevertheless, these are the only factors known to affect amide exchange from polypeptides that can account for shifts of pH_{min} to high pH in a peptide containing only positively charged side chains.

ACKNOWLEDGMENTS

I am grateful to the Oxford Enzyme Group for access to the NMR spectrometers, to Dr. Trevor Poile for computer programming, to Drs. R. Bazzo, I. Campbell, A. Pastore, A. Rosenberg, M. Tappin, and C. Woodward for valuable discussion, and to Frank Caddick for drawing some of the figures.

Registry No. PDLA, 25281-63-4; MeOH, 67-56-1; O_2, 1333-74-0; D_2, 7782-39-0; melittin, 20449-79-0.

REFERENCES

Atkins, P. W. (1986) *Physical Chemistry*, 3rd ed., Oxford University Press, Oxford.

Banks, B. E. C., Dempsey, C. E., Pearce, F. L., Wholley, T. E., & Vernon, C. A. (1981) *Anal. Biochem. 116*, 48–52.

Bates, R. G. (1973) *Determination of pH; Theory and Practice*, Wiley, New York.

Bates, R. G., Pabo, M., & Robinson, R. A. (1963) *J. Phys. Chem. 67*, 1833–1838.

Bazzo, R., Tappin, M. J., Pastore, A., Harvey, T. S., Carver, J. A., & Campbell, I. D. (1988) *Eur. J. Biochem. 173*, 139–146.

Blundell, T., Barlow, D., Borkakoti, N., & Thornton, J. (1983) *Nature (London) 306*, 281–283.

Chou, P. Y., & Fasman, G. D. (1974a) *Biochemistry 13*, 211–222.

Chou, P. Y., & Fasman, G. D. (1974b) *Biochemistry 13*, 222–245.

Creighton, T. E. (1983) *Biopolymers 22*, 49–58.

Dawson, C. R., Drake, A. F., Helliwell, J., & Hider, R. C. (1978) *Biochim. Biophys. Acta 510*, 75–78.

de Ligney, C. L. Luykx, P. F. M., Rehbach, M., & Wieneke, A. A. (1960) *Recl. Trav. Chim. Pays-Bas 79*, 713–730.

Dempsey, C. E. (1986a) *Biochemistry 25*, 3904–3911.

Dempsey, C. E. (1986b) *Eur. J. Biochem. 157*, 617–618.

Douheret, G. (1967) *Bull. Soc. Chim. Fr. 4*, 1412–1419.

Englander, J. J., Calhoun, D. B., & Englander, S. W. (1979) *Anal. Biochem. 92*, 517–524.

Englander, S. W., & Kallenbach, N. (1984) *Q. Rev. Biophys. 16*, 521–655.

Fox, R. O., & Richards, F. M. (1982) *Nature (London) 300*, 325–330.

Gutbezahl, B., & Grunwald, E. (1953) *J. Am. Chem. Soc. 75*, 565–574.

Habermann, E., & Jentsch, J. (1967) *Hoppe-Seyler's Z. Physiol. Chem. 348*, 37–50.

Henry, G. D., Weiner, J. H., & Sykes, B. D. (1987) *Biochemistry 26*, 3626–3634.

Hol, W. G. L. (1985) *Prog. Biophys. Mol. Biol. 45*, 149–195.

Hvidt, A., & Nielsen, S. O. (1966) *Adv. Protein Chem. 21*, 287–386.

Kim, P. S., & Baldwin, R. L. (1982) *Biochemistry 21*, 1–5.

Kuwajima, K., & Baldwin, R. L. (1983) *J. Mol. Biol. 169*, 299–322.

Leichtling, B., & Klotz, I. (1966) *Biochemistry 5*, 4026–4037.

Matthew, J. B., & Richards, F. M. (1982) *Biochemistry 21*, 4989–4999.

Matthew, J. B., & Richards, F. M. (1983) *J. Biol. Chem. 258*, 3039–3044.

Matthew, J. B., Gurd, F. R. N., Garcia-Moreno, B. E., Flanagan, M. A., March, K. L., & Shire, S. J. (1985) *CRC Crit. Rev. Biochem. 18*, 91–197.
Molday, R. S., & Kallen, R. G. (1972) *J. Am. Chem. Soc. 94*, 6739–6745.
Molday, R. S., Englander, W. S., & Kallen, R. G. (1972) *Biochemistry 11*, 150–158.
Nakanishi, M., Masamichi, T., Ikegami, A., & Kanehisa, M. (1972) *J. Mol. Biol. 64*, 363–378.
Perrin, C., & Lollo, C. (1984) *J. Am. Chem. Soc. 106*, 2754–2757.
Schellman, J. A. (1955) *C. R. Trav. Lab. Carlsberg, Ser. Chim. 29*, 230–259.
Terwilliger, T. C., & Eisenberg, D. (1982) *J. Biol. Chem. 257*, 6016–6022.
Terwilliger, T. C., Weissman, L., & Eisenberg, D. (1982) *Biophys. J. 37*, 353–359.
Tuchsen, E., & Woodward, C. (1985) *J. Mol. Biol. 185*, 421–430.
Vasant Kumar, N., & Kallenbach, N. R. (1985) *Biochemistry 24*, 7658–7662.
Wagner, G., Stassinopoulou, C. I., & Wuthrich, K. (1984) *Eur. J. Biochem. 145*, 431–436.
Wand, A. J., Roder, H., & Englander, S. W. (1986) *Biochemistry 25*, 1107–1114.
Wemmer, D., & Kallenbach, N. R. (1983) *Biochemistry 22*, 1901–1906.
Woodward, C., Simon, I., & Tuchsen, E. (1982) *Mol. Cell. Biochem. 48*, 135–160.

Nested Allosteric Interaction in Tarantula Hemocyanin Revealed through the Binding of Oxygen and Carbon Monoxide†

Heinz Decker,‡ Patrick R. Connelly,§ Charles H. Robert,§ and Stanley J. Gill*,§

Department of Chemistry and Biochemistry, University of Colorado, Boulder, Colorado 80309-0215, and Zoologisches Institut, Universitat Munchen, 8 Munchen 2, FRG

Received December 17, 1987; Revised Manuscript Received April 19, 1988

ABSTRACT: We have examined the competitive binding of oxygen and carbon monoxide to the multisubunit hemocyanin of the tarantula *Eurypelma californicum*. Employment of high-precision thin-layer methods has enabled detailed characterization of the pure oxygen and pure carbon monoxide binding curves, as well as binding curves performed under mixed-gas conditions. The pure oxygen binding curve and the displacement of oxygen by carbon monoxide at full ligand saturation are highly cooperative, but in the absence of oxygen, carbon monoxide binds noncooperatively. The results were analyzed globally within the framework of a *nested allosteric model* [Robert, C. H., Decker, H., Richey, B., Gill, S. J., & Wyman, J. (1987) *Proc. Natl. Acad. Sci. U.S.A. 84*, 1891–1895] which takes into account the hierarchy of subunit structure present in the macromolecule. The use of two ligands enables one to recognize two distinct levels of allosteric interaction functioning in the protein assembly. The binding characteristics of the allosteric states demonstrated for *Eurypelma* follow a similar pattern as those found earlier for *Homarus americanus*.

Hemocyanins are large multisubunit proteins that provide for oxygen transport in many species of arthropods and mollusks. Among the properties of hemocyanins that motivate a study of the thermodynamics of their binding reactions are the following: (1) functionally, they display highly cooperative behavior in binding oxygen (Van Holde & Miller, 1982), and (2) structurally, they reveal hierarchies of subunit organization typical of many macromolecular complexes found in biological systems (Robert et al., 1987; Wyman, 1972). In arthropods the basic structural element is a hexamer. Various species have been reported to have structures consisting of a single hexamer, a single dimerized aggregate of a hexamer (dodecamer), and higher aggregates composed of two or four dodecamers (Van Holde & Van Bruggen, 1971; van Bruggen et al., 1982; Markl, 1986). The general notion that the hierarchy of structure present in large macromolecules is reflected in a corresponding hierarchy of function through allosteric interaction was introduced by Wyman and has been termed "nesting" (Wyman, 1985, 1972). More recently, it has been described in a quantitative manner in regard to hemocyanins (Robert et al., 1987).

Among arthropod hemocyanins, that of the tarantula, *Eurypelma californicum*, has been the subject of extensive structural investigations which reveal that it has 24 subunits arranged as a dimer of isologous dodecamers (Markl et al., 1981a,b). Each dodecamer is composed of seven different types of subunits (Markl et al., 1982). In addition, the crystal structure of a closely related hexameric arthropod hemocyanin from the spiny lobster, *Panulirus interruptus*, has been determined at a resolution of 3.2 Å (Gaykema et al., 1984, 1986). The reaction of *Eurypelma* hemocyanin with oxygen is highly cooperative. Hill slopes exceeding 7 have been reported (Loewe et al., 1977; Loewe, 1978; Decker, 1981), making it one of the most cooperative of any binding system studied. In contrast to oxygen binding, carbon monoxide binds to arthropod hemocyanins noncooperatively or with only slight positive cooperativity, and with a much lower affinity than oxygen (Bonaventura et al., 1974; Brunori et al., 1981; Richey et al., 1985). Such markedly different binding behavior of

†This work was supported by National Institutes of Health Grant HL22325 (S.J.G.) and Deutsche Forschungsgesellschaft (Li 107/24-8) (H.D.).
‡Universitat Munchen.
§University of Colorado.

0006-2960/88/0427-6901$01.50/0